The Effects of Lateral Eccentricity on Failure Loads and Injuries of the Cervical Spine in Head-First Impacts

C. Van Toen[1,3], A.D. Melnyk[1,3], J. Street[2,3], T.R. Oxland[1,3], P.A. Cripton[1,3]
[1]Orthopaedic & Injury Biomechanics Group, University of British Columbia;
[2]Combined Neurosurgical & Orthopaedic Spine Program, University of British Columbia;
[3]International Collaboration on Repair Discoveries (ICORD), Vancouver BC

ABSTRACT

Current neck injury criteria do not include limits for lateral bending combined with axial compression and this has been observed as a clinically relevant mechanism, particularly for rollover motor vehicle crashes. The primary objectives of this study were to evaluate the effects of lateral eccentricity (the perpendicular distance from the axial force to the centre of the spine) on peak loads, kinematics, spinal canal occlusions, and structural injury patterns of subaxial cervical spine specimens tested in dynamic axial compression (0.5 m/s). Thirteen 3-vertebra human cadaver cervical spine specimens (6 C3-5, 3 C4-6, 2 C5-7, 2 C6-T1) were tested in two groups: low and high eccentricity with initial eccentricities of 1% and 150% of the lateral diameter of the vertebral body. Six-axis loads inferior to the specimen, kinematics of the superior-most vertebra, and spinal canal occlusions were measured. The effects of eccentricity on peak loads, kinematics, and canal occlusions were evaluated using unpaired Student t-tests. Injuries were diagnosed by a spine surgeon and scored. Classification functions were developed using discriminant analysis. The high eccentricity group had lower peak axial forces (1544 ±629 vs. 4296 ±1693 N), inferior displacements (0.2 ±1.0 vs. 6.6 ±2.0 mm), and canal occlusions (27 ±5 vs. 53 ±15%) and higher peak ipsilateral bending moments (53 ±17 vs. 3 ±18 Nm), ipsilateral bending rotations (22 ±3 vs. 1 ±2^{o}), and ipsilateral displacements (4.5 ±1.4 vs. -1.0 ±1.3 mm, $p<0.05$ for all comparisons). Low and high eccentric loading resulted in primarily bony fractures and soft tissue injuries, respectively. The developed classification functions had 92% classification accuracy. Dynamic axial compression loading of the cervical spine with high lateral eccentricities produced lower canal occlusions and primarily soft tissue injuries while loading with low eccentricities produced greater canal occlusions and primarily bony fractures. These results provide new insights to develop prevention, recognition, and treatment strategies for compressive cervical spine injuries with lateral eccentricities.

INTRODUCTION

Current injury criteria for the cervical spine, which are used to evaluate the efficacy of airbags and seatbelts, define loads that represent thresholds of injury to the spinal column (Eppinger et al. 2000; Mertz et al. 2003). Limits for loading in flexion, extension, axial compression, and tension are enshrined in government automotive safety regulations and these are based on experimental testing and accident reconstructions (Mertz and Patrick 1971; Mertz et al. 1978; Nyquist et al. 1980; Prasad and Daniel 1984). However, corresponding limits for lateral bending are not in use by government standards and the moment limits that have been suggested are simply the average of those in flexion and extension (Mertz et al. 2003). Lateral bending of the cervical spine occurs in side impact motor vehicle collisions (Kallieris and Schmidt 1990) and experimental studies have indicated that lateral bending may occur simultaneously with axial compression during rollover motor vehicle crashes (MVCs) (Bahling et al. 1990). Real world head-first impacts in sports often appear to involve lateral bending of the cervical spine in video replays. It is, thus, conceivable that lateral bending may be present in real-world axial loading events. This indicates a need for further understanding of the tolerance of the cervical spine in lateral bending.

Axial loading of the cervical spine is the primary mechanism leading to spine and spinal cord injury in football, diving, hockey, and rollover motor vehicle accidents (Bahling et al. 1990; Bailes et al. 1990; Torg et al. 2002; Tator et al. 2004; Thompson et al. 2009). Although theories and information abound for the influence of combined sagittal plane bending (Allen et al. 1982; White and Panjabi 1990; Myers and Winkelstein 1995), there is a lack of information about combined coronal plane bending. "Lateral flexion" injuries to the cervical spine are well recognized in clinical practice (Roaf 1963; Chrisman et al. 1965; Schaaf et al. 1978; Scher 1981) and clinical studies have hypothesized lateral bending in combination with other loads as mechanisms for unilateral injuries (Allen et al. 1982; White and Panjabi 1990; Halliday et al. 1997; Lifeso and Colucci 2000; Lee and Sung 2009). However, the role of lateral bending in producing some unilateral injuries is unclear (Allen et al. 1982; White and Panjabi 1990; Myers and Winkelstein 1995). The most likely injuries to result from axial compression combined with lateral bending are unknown and this knowledge could assist in elucidating mechanisms of other unilateral injuries.

Numerous experiments have investigated the response of the cervical spine to lateral bending without an external compression force (Gadd et al. 1971; Patrick and Chou 1976; Kallieris and Schmidt 1990; Kettler et al. 2004; McIntosh et al. 2007; Yoganandan et al. 2009; Yoganandan et al. 2011); however, very few studies have evaluated the cervical spine in lateral bending with combined axial compression (Selecki and Williams 1970; Toomey et al. 2009). Due to this paucity of data, the tolerance and injury mechanisms of the cervical spine in compression-lateral bending are not well understood. An understanding of these mechanisms is essential for advancing injury prevention approaches such as helmets, neck protectors, and automotive restraints and to facilitate recognition of clinical injury patterns that would guide surgical treatment.

The primary objectives of this study were to evaluate the effects of lateral eccentricity (perpendicular distance from the axial force to the centre of the spine) on peak loads, kinematics, spinal canal occlusions, and structural injury patterns of subaxial cervical spine specimens tested in dynamic axial compression.

METHODS

Specimens

Eleven fresh-frozen human cadaveric cervical spines were obtained and stored at -20^{o}C until use. Specimens were separated into 13 three-vertebra segments and they were dissected free from musculature while the ligaments and intervertebral discs (IVDs) were preserved (Tables 1, 2). The coronal and sagittal diameters of the superior-(cranial) and inferior-most (caudal) vertebral bodies and specimen heights were measured using vernier calipers. Specimens were scanned with CT (Xtreme CT, Scanco Medical, Brüttisellen, Switzerland, resolution 246 µm) before and after testing. Specimens were potted in polymethylmethacrylate (PMMA) (Figure 1), such that a line through the points in the sagittal plane representing the approximate instantaneous axes of flexion-extension rotation of the superior and inferior functional spinal units was vertical (Amevo et al. 1991).

Table 1: Summary of the specimen and donor details for the low eccentricity group (1% of the average lateral dimension of the cranial and caudal vertebral bodies) as well as the major injuries experienced by these specimens. 'NA' indicates that the data was not available. Specimens H1275 (Table 2) and H1975 were from the same donor and specimens H1298 and H1998 (Table 2) were from the same donor. For the specimens marked with *, donor genders were determined using DNA (deoxyribonucleic acid) microsatellite analysis performed on donor muscle tissue. EP: endplate fracture, FJ: articular facet fracture, inf: inferior, LAM: lamina fracture, sup: superior, V1: superior vertebra, V2: middle vertebra, VB: vertebral body fracture, VBA: vertebral body area.

Specimen Number	**Level**	**Age, Gender**	**Initial Eccentricity (mm)**	**Major Injuries**
H1318	C57	72, F	0.3	V1: EP (inf), VB
H1323	C35	NA, M	0.3	V2: EP (sup), VB, LAM
H1321	C46	72, M	0.3	V2: EP (sup), VB
H1298	C35	68, F	0.3	V2: EP (sup), LAM
H1975	C6T1	79, M	0.3	V2: EP (sup & inf), VB
H1274	C35	78, M	0.2	V1: VB V2: FJ (sup)
H1052	C35	74, M*	0.3	V1: VB, V2: EP (sup & inf), VB, V3: EP (sup)
Average (standard deviation)		74 (4)	0.3 (0.04)	

Table 2: Summary of the specimen and donor details for the high eccentricity group (150% of the average lateral dimension of the cranial and caudal vertebral bodies) as well as the major injuries experienced by these specimens. 'NA' indicates that the data was not available. Specimens H1275 and H1975 (Table 1) were from the same donor and specimens H1298 (Table 1) and H1998 were from the same donor. For the specimens marked with *, donor genders were determined using DNA (deoxyribonucleic acid) microsatellite analysis performed on donor muscle tissue. ALL: anterior longitudinal ligament tear, EP: endplate fracture, FC: facet capsule tear, inf: inferior, ISL: interspinous ligament tear, IVD: intervertebral disc injury, LF ligamentum flavum tear, PLL: posterior longitudinal ligament tear, sup: superior, V1: superior vertebra, V2: middle vertebra, V3: inferior vertebra, VB: vertebral body fracture, VBA: vertebral body area.

Specimen Number	**Level**	**Age, Gender**	**Initial Eccentricity (mm)**	**Major Injuries**
H1125	C46	NA, M*	39.9	V2/3: FC, LF, ALL, IVD
H1329	C57	NA, M*	48.1	V2/3: FC, LF, ISL, ALL, PLL, IVD
H1275	C35	79, M	41.4	V2/3: FC, LF, ISL, ALL, PLL, IVD; V2: VB
H1286	C46	66, F	38.3	V1/2: FC, LF, ISL, ALL, PLL, IVD; V2: EP (sup)
H1998	C6T1	68, F	43.6	V2/3: FC, LF, ISL, ALL, IVD; V2: EP (inf); V3: EP (sup)
H1292	C35	67, M	42.6	V2/3: FC, LF, ISL, ALL, PLL, IVD; V2: EP (inf); V3: EP (sup)
Average (standard deviation)		70 (6)	42.3 (3.4)	

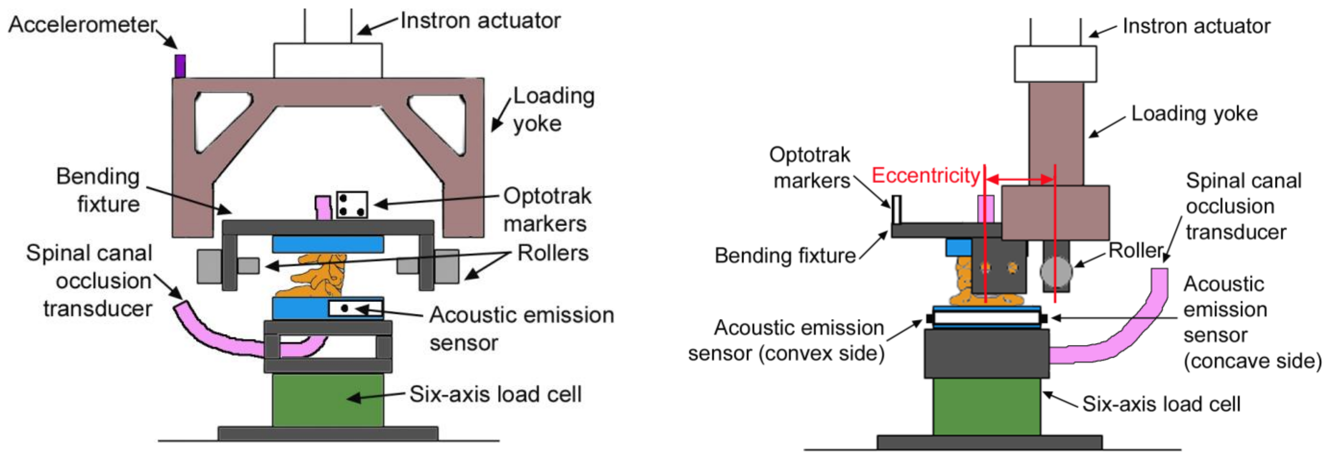

Figure 1: Schematics of the custom loading apparatus with lateral bending rotation and lateral displacement unconstrained: lateral (A) and anterior (B) views. The loading yoke is connected to the Instron actuator and the bending fixture, with rollers located anterior and posterior to the specimen at the approximate axial location of the middle vertebra, is connected to the specimen. Prior to the loading process, the loading yoke and rollers are in contact. During the loading process, the loading yoke is lowered and the rollers roll laterally on the loading yoke as the specimen rotates laterally. The Optotrak (infrared) markers, spinal canal occlusion transducer, and six-axis load cell are also shown.

Loading

A custom loading apparatus was used (Figure 1), which consisted of two bearing rollers (model CF-1-S, McGill Mfg Co, Valparaiso IN) that were placed anterior and posterior to the specimen, equidistant from the geometric centre of the inferior IVD. Preload was applied to specimens, through the loading yoke and bending fixture (Figure 1), as the actuator of a servohydraulic materials test system (model 8874, Instron, Canton MA) was lowered until a compression force of 50 N was reached and this displacement was held constant for approximately six minutes. Specimens were then tested in dynamic eccentric axial compression to a set displacement at a rate of 0.5 m/s, held at this position for 0.1 s, and unloaded at a rate of 50 mm/s using the servohydraulic materials test system. Although an impact velocity of 3 m/s is generally considered to be the minimum required to result in clinically relevant cervical spine injuries in head-first impacts (McElhaney et al. 1979; Nightingale et al. 1996), this rate is expected to be distributed across all levels of the cervical spine and reduced velocities are thought to be relevant for small segment testing (Edwards 1998; Carter 2002). Specimens were randomly assigned to one of two test groups: low or high eccentricity, where the eccentricities (randomly assigned to the right or left) were set to 1% and 150% of the average lateral dimension of the cranial and caudal vertebral bodies, respectively. These eccentricities were selected to represent the extremes possible in head-first impacts, based on the dimensions of the head (Walker et al. 1973), and these were within the range of those used in eccentric sagittal plane axial loading (Maiman et al. 2002). Specimens in the low and high eccentricity groups were compressed to 20% and 40% of their height (vertical distance from the inferior-most to superior-most aspect of the vertebral bodies while in the potting orientation), respectively. This increased magnitude of compression for the high eccentricity group was selected to allow for physiologic, non-injurious lateral bending rotation that occurred in this loading mode. Before and after dynamic loading, specimens underwent flexibility testing to a maximum moment of 1.5 Nm in flexion/extension, lateral bending, and axial rotation. These results are described elsewhere (Van Toen 2013; Van Toen et al. 2014b).

Data Collection

An accelerometer (range 500 g, model 355B02, PCB Piezotronics, Depew NY) was mounted to the superior loading fixture for inertial compensation of the Instron load. Acceleration and load and displacement from the Instron were collected at 2.5 MHz. Six-axis loads were measured using a load cell placed inferior to the specimen (range 13 kN, 452 Nm flexion-extension and lateral bending, 226 Nm axial rotation, model 4366J, Denton ATD, Inc., Rochester Hills NJ) and collected at 50 kHz. Three infrared light emitting diodes were attached to the superior mounting block to obtain upper vertebra kinematics and their positions were collected at 920 Hz with an optoelectronic camera system (Certus, Optotrak, Waterloo ON, Canada). High speed videos of the tests were recorded using two cameras at 6,400 frames per second (resolution 480 x 480 pixels, Phantom v9, Vision Research, Wayne NJ) located on the left and right sides of specimens. Acoustic emission signals were also collected; however these details are described elsewhere (Van Toen 2013; Van Toen et al. 2014a).

A custom designed spinal canal occlusion transducer (SCOT) was used to measure the changes in cross sectional area of the spinal canal (Raynak et al. 1998; Zhu et al. 2008). Four voltages were collected from the SCOT at 20 kHz, corresponding to four sensing segments in the spinal canal. The functional range of the transducer was from a total outside area of 198.6 mm^2 to 99.5 mm^2. The accuracy of the SCOT was 8 mm^2, for a 10 mm square impactor, and its sensitivity to impactor size was 14 mm^2. The tube of the SCOT sensor (outer diameter 15.9 mm) fit snugly into the spinal canal of the specimens (average sagittal diameter 13.9 (SD 1.3) mm).

Data Analysis

Moments were resolved to those at the geometric centre of the inferior-most IVD (Carter et al. 2002). Force, displacement, and acceleration data were low-pass filtered (fourth order, zero phase, cutoff 1 kHz). Kinematic data calculated from the optical marker positions were resolved to those of the anterior-inferior edge of the superior-most vertebra. SCOT signals were also low-pass filtered (fourth order, zero phase, cutoff 120 Hz) (Raynak 2000). For each segment, percent SCOT occlusion was defined using a normalized cross sectional area as follows (Zhu et al. 2008):

$$Percent\ SCOT\ Occlusion\ (t) = (A_o - A(t))/(A_o - 70.6) \times 100$$

where A(t) is the outside area of the tube at time t, and A_o is the initial outside area measured prior to impact for each specimen. All post-processing and analyses were performed using Matlab (version 7.8, Mathworks Inc., Natick MA).

Unpaired Student t-tests with the significance level at 95% were used to evaluate differences in peak axial forces, lateral bending moments and rotations, inferior and lateral displacements, and SCOT occlusions.

Injury Scoring

Injuries were diagnosed by a fellowship-trained spine surgeon (author JS) through evaluation of the post-test CT scans and through post-test anatomic dissection. Initial injuries were diagnosed, which were then confirmed or disproved through dissection. The superior, middle, and inferior vertebrae were referred to as V1, V2, and V3, respectively. Anatomic structures representing hard tissues were divided into left, middle (i.e. midline), and right components and those representing soft tissues were divided into left and right sides (Figure 2A, 2B). This resulted in a total of 50 anatomic structures that were examined, each consisting of two, three, or five anatomic components.

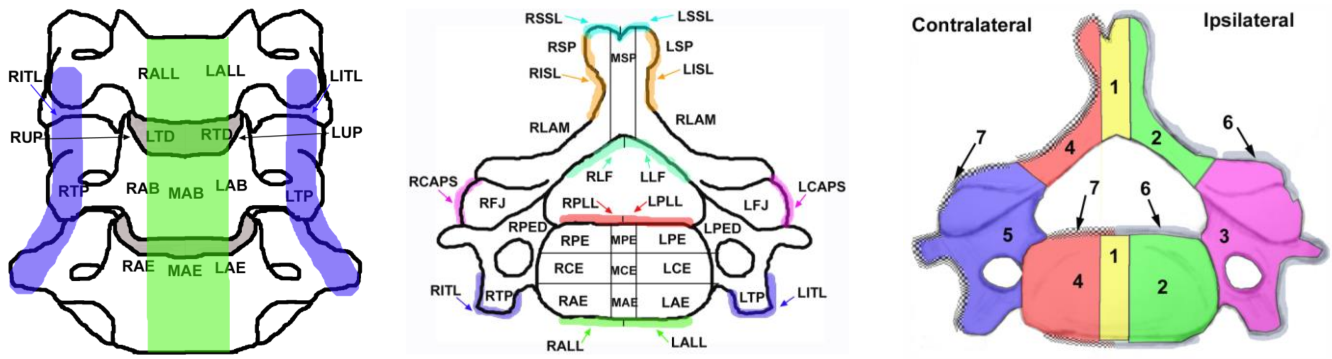

A B C

Figure 2: (A, B) Schematic diagrams of three-vertebra segments of the lower cervical spine illustrating some of the anatomic structures examined: (a) anterior and (b) superior views. (c) Schematic diagram of a cervical vertebra illustrating the division of anatomic structures into groups (Table 3). This schematic is for a specimen tested with a left lateral eccentricity (ipsilateral structures are indicated on the left side of the specimen).

Anatomic components that were intact, partially injured (soft tissue fibers partially intact, trabecular voids present in vertebral bodies, or incomplete fracture of remaining hard tissues), and completely injured (soft tissue fibers completely torn, fractured vertebral bodies, or complete fracture of remaining hard tissues) were given scores of 0, 1, and 2, respectively. The score of each of the 50 anatomic structures was the sum of its anatomic component scores. Anatomic structures were also collected into seven groups for further analysis (Table 3, Figure 2C). Group scores were calculated by adding the scores of all the anatomic structures in each. Group scores were then normalized by dividing each by the highest score for that group occurring in all specimens and multiplying this value by 10 for a final score between 0 and 10.

Table 3: Summary of anatomic groups (Figure 2C), columns, tissue types, and anatomic structures. VB: vertebral body, EP: endplate, LAM: lamina, SP: spinous process, TP: transverse process, UP: uncinate process, PED: pedicle, FJ: articular facet, LM: lateral mass, ALL: anterior longitudinal ligament, TDI: transdiscal injury, PLL: posterior longitudinal ligament, ITL: intertransverse ligament, CAPS: facet capsular ligament, LF: ligamentum flavum, ISL: interspinous ligament, SSL: supraspinous ligament.

Group	Column	Tissue Type	Anatomic Structures
1	Midline	Hard	VB, EP, LAM, SP
2	Ipsilateral-Medial	Hard	VB, EP, LAM, SP
3	Ipsilateral-Lateral	Hard	TP, UP, PED, FJ, LM
4	Contralateral-Medial	Hard	VB, EP, LAM, SP
5	Contralateral-Lateral	Hard	TP, UP, PED, FJ, LM
6	Ipsilateral	Soft	ALL, TDI, PLL, ITL, CAPS, LF, ISL, SSL
7	Contralateral	Soft	ALL, TDI, PLL, ITL, CAPS, LF, ISL, SSL

In order to determine classification equations indicating the impact eccentricity given the structures injured, a discriminant analysis was performed on the logarithm transformed group injury scores (Carter 2002). This transformation was performed for unequal variances of the data. Classification accuracy was calculated as the number of specimens properly classified by these equations divided by the total number of specimens and multiplied by 100. The strength of the classification equations was evaluated using jack-knife cross-validation (Afifi and Clark 1996). A cross-validation rate was calculated, which is the number of specimens properly reclassified divided by the total number of specimens, and multiplied by 100 and an assessment of the significance of this rate was performed using methods described by Sharma (Sharma 1996).

RESULTS

Kinematic data was not collected for one specimen in the low eccentricity group (H1052). Dynamic data from this specimen (kinetic, kinematic and SCOT data) were omitted from further analysis.

Peak axial forces for the low eccentricity group were greater than those for the high eccentricity group (Figure 3). Peak ipsilateral lateral bending moments (in the same direction as the eccentricity) were greater for the high eccentricity group than the low eccentricity group and these were up to 80 Nm for the high eccentricity group.

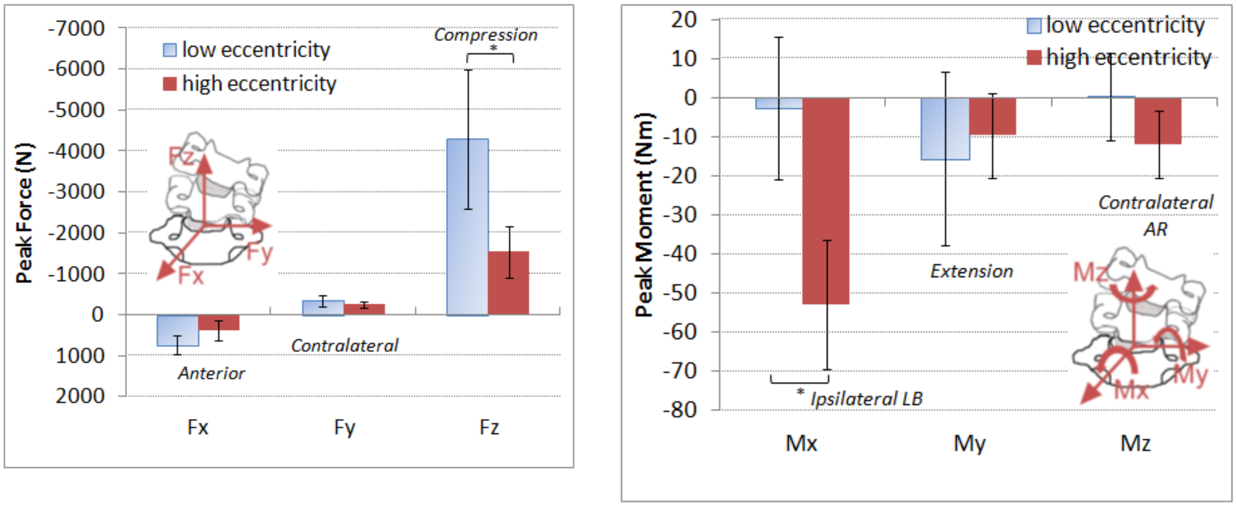

A B

Figure 3: Average peak forces (A) and moments (B) are also indicated (bars indicate ± 1 standard deviation). The coordinate system for loads is indicated in the inset images. Statistically significant differences are shown with *.

Due to the excessive lateral bending rotation of the specimens in the high eccentricity group, kinematic data could not be collected for two specimens after the time of peak axial force (H1275, H1329); values at the time of peak axial force were compared. Specimens rotated primarily in lateral bending, with small rotations in flexion-extension and axial rotation (Figure 4). Ipsilateral lateral bending rotations (in the same direction as the eccentricity) at the time of peak force for the high eccentricity group were greater than those for the low eccentricity group. Ipsilateral displacements were greater and inferior displacements were lesser for the high eccentricity group than for the low eccentricity group (Figure 4).

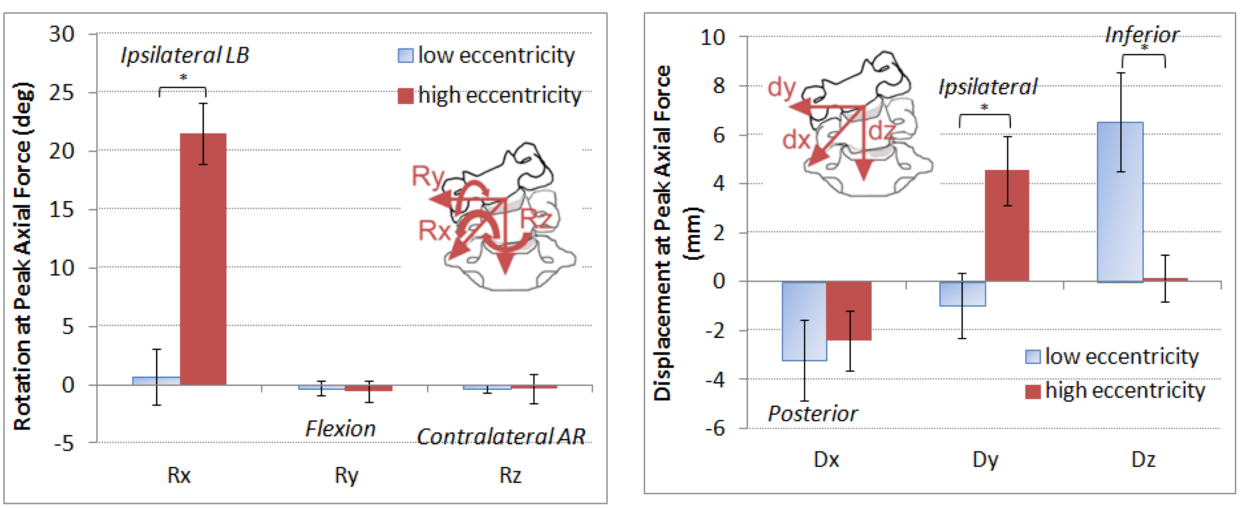

A B

Figure 4: Average rotations (A) and displacements (B) at peak axial load are also indicated (bars indicate ± 1 standard deviation). The coordinate system for kinematics is indicated in the inset images. Statistically significant differences are shown with *.

Erroneous SCOT data, which contained transient DC shifts, were collected for the superior-most segment in three of the specimens in the high eccentricity group (H1329, H1275, and H1292). These signals were omitted from further analysis. SCOT occlusions increased with time after impact the initiation of loading and the measuring segments with the highest values corresponded to spinal levels where there were fractures or dislocations. Peak SCOT occlusions, up to 76% and 33% for the low and high eccentricity groups, respectively were greater for specimens in the low eccentricity group (Figure 5).

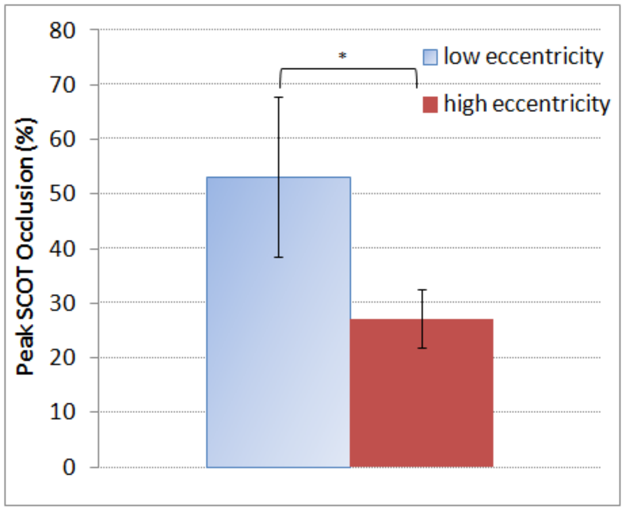

Figure 5: Average SCOT occlusions for the low and high eccentricity groups (bars indicate ± 1 standard deviation). This difference was statistically significant.

Specimens in the low eccentricity group failed primarily through bony fractures, in particular, those of the vertebral bodies and endplates with fractures of the laminae and spinous processes on the ipsilateral side (Figure 6A). Two such specimens had burst-type fractures (H1975 and H1323). Specimens in the high eccentricity group failed primarily through contralateral soft tissue injury (Figure 6B).

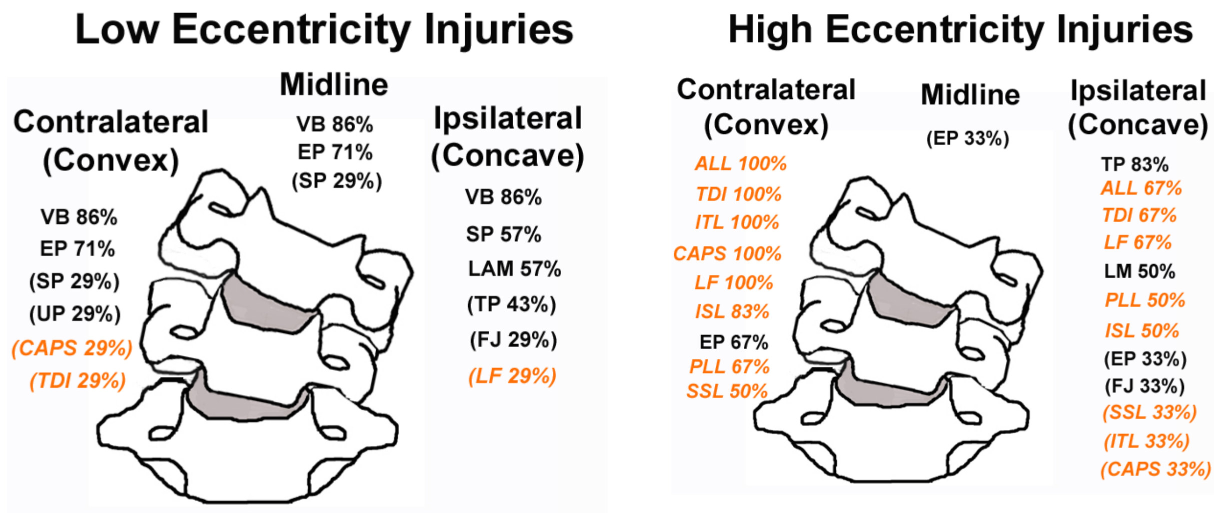

A B

Figure 6: Schematic diagrams indicating the structures injured for specimens in the low (A) and high (B) eccentricity groups. The percentage of specimens that had one or more injury of each type on the convex, concave, or midline aspects of the specimen are shown. Orange italicized text indicates soft tissue injuries and black text indicates hard tissue injuries. The injuries and numbers in brackets indicate that less than 50% of the specimens had injuries of this type in this location. Injuries that only occurred on one specimen (frequency less than 20%) are not indicated in this figure. ALL: anterior longitudinal ligament, CAPS: facet capsule, EP: endplate, FJ: facet joint, ISL: interspinous ligament, ITL: intertransverse ligament, LAM: lamina fracture, LF: ligamentum flavum, LM: lateral mass, PLL: posterior longitudinal ligament, SP: spinous process, SSL: supraspinous ligament, TDI: transdiscal injury, TP: transverse process, UP: uncinate process, VB: vertebral body.

The discriminant analysis showed a statistically significant discrimination between groups and that injury groups 7 (contralateral soft tissue) and 4 (contralateral-medial hard tissue) were the best discriminators for applied eccentricity ($p<0.0004$). Classification functions were determined and these had a 92% classification accuracy (Table 4). The cross validation rate was 85% and this was significant, indicating a low probability of achieving this rate due to random chance ($p=0.013$).

Table 4: Classification functions determined using discriminant analysis. A specimen would be classified into the group with the highest resulting function (i.e. if the high eccentricity function produced a higher value than the low eccentricity function, the specimen would be classified into the high eccentricity group).

$low\ ecc = 2.98 \times transformed\ group\ 7\ score + 6.42 \times transformed\ group\ 4\ score - 3.2$
$high\ ecc = 18.83 \times transformed\ group\ 7\ score + 2.58 \times transformed\ group\ 4\ score - 10.01$

DISCUSSION

There is a paucity of biomechanical information available for compression-lateral bending loading of the cervical spine and this is of recent interest, particularly for interpreting results of experimental (Moffatt et al. 2003) and computational (Hu et al. 2008) studies of rollover MVCs. To our knowledge, very few studies have experimentally evaluated this injury mechanism (Selecki and Williams 1970; Toomey et al. 2009) and injurious lateral bending moments have only been reported for two specimens (Toomey 2012). Information on the kinetics, kinematics, and associated risk of injury to the spinal cord for this failure mode may be important to improve injury criteria and assist in the development of safety devices. In addition, this information could also be extrapolated to the clinical setting where advanced understanding of injury mechanisms could direct surgical planning and treatment and perhaps prognosticate for recovery of spinal cord injury.

In axial compression, higher lateral eccentricities resulted in lower peak axial forces and higher peak lateral bending moments. Yoganandan et al. fixed the heads of two cadaver specimens to a rotational actuator, which produced up to 74 Nm lateral bending moments at the occipital condyles and up to 400 N compression forces without injury (Yoganandan et al. 2011). These moments are comparable to those of the high eccentricity group in the present study (up to 80 Nm) with lower compression forces (up to 2599 N). These results are consistent with the spine being able to tolerate larger bending moments with decreased axial forces, as reflected by the (current sagittal plane only) Nij injury criteria (Eppinger et al. 2000).

Based on the present occlusion data, low eccentricity impacts are more likely to be associated with spinal cord injury (SCI) than high eccentricity impacts. Using a simplified geometric representation of the spinal canal to relate the occlusions to spinal cord compressions, an average low eccentricity load would be expected to result in a mild to moderate extent of SCI while it was unlikely that our high eccentricity loads would result in SCI (Kearney et al. 1988). It is thought that in cases of fracture, bone fragments are projected towards the cord and this results in the high SCOT occlusions recorded.

Low and high lateral eccentricity loading resulted in primarily hard and soft tissue injuries, respectively, and these types of injuries are also observed clinically (Schaaf et al. 1978; Scher 1981; Allen et al. 1982). As the soft tissue injuries resulting from high eccentricity impacts are associated with increased spinal flexibilities (Van Toen 2013; Van Toen et al. 2014b), it is likely that these impacts result in less clinically stable spines, indicating that post-trauma care including immobilization would be vital for patients with these injuries.

For axial impact loading of the cervical spine, it is believed clinically (Allen et al. 1982) and it has been shown experimentally (Southern et al. 1990; Carter 2002) that injuries vary with anteroposterior eccentricities. Similarly, it is expected that compressive cervical spine injuries would vary with lateral eccentricities. What is known about the spectrum of injuries with varying levels of lateral eccentricity may be evaluated based on the present results in context with results from studies aligned axial force that effectively use an eccentricity of zero (Southern et al. 1990; Zhu et al. 1999; Carter 2002), medium levels of lateral eccentricity (Selecki and Williams 1970; Toomey et al. 2009), and those applying lateral impacts or coronal head rotations, which may be considered to be equivalent to axial loads applied at very large lateral eccentricities (Horsch et al.

1979; Klaus and Kallieris 1983; Kallieris and Schmidt 1990; Kallieris et al. 1996; Hartwig et al. 2004; Kettler et al. 2004; McIntosh et al. 2007; Yoganandan et al. 2009). These data are consistent with larger lateral eccentricities producing primarily soft tissue injuries and fractures of more laterally located structures and smaller lateral eccentricities producing fractures of more medial structures. Additional specimens tested at intermediate levels of lateral eccentricity are needed to confirm this hypothesis.

Although muscle forces likely resist lateral bending *in vivo*, we tested short segments of the osteoligamentous spine in this important initial *ex vivo* evaluation of the influence of lateral bending on cervical spine injury in axial loading. This allowed us to focus directly on the basic injury mechanisms and failure loads of the spinal unit with a minimum of confounding factors. The lack of muscle forces may have specifically altered the presence of transverse process fractures, as these are also thought occur due to muscle tension on the convex side (Scher 1981). The use of short segments, which are widely used to study spine injury mechanisms (Moroney et al. 1988; Shea et al. 1991; Crowell et al. 1993; Pintar et al. 1995; Carter et al. 2002; Nightingale et al. 2007; Przybyla et al. 2007), allowed us to examine injury mechanisms in a repeatable fashion and to measure loads near the site of injury. As specimens were obtained from donors with relatively advanced ages, caution should be used when applying the present results to younger populations. Our mechanism for producing injuries allowed for only minimal axial rotation and flexion-extension motions and these might occur to a greater extent during injuries to the *in vivo* spine, however this allowed us to focus on the influence of lateral bending on compressive cervical spine injuries in a relatively isolated sense. The classification functions provide a tool that clinicians and researchers could use to study the influence of lateral bending in real-world injuries. However, the present functions are limited as they have not been tested against additional specimens. The limitations of the SCOT sensor include that it did not fill the entire spinal canal for all specimens, particularly laterally. Although this might have led to underestimated canal occlusions, it is noteworthy that, mediolaterally, the spinal cord occupies the central third of the subaxial canal and so occlusions in the lateral-most space are likely to be of less clinical interest. Such far-lateral compression is more likely to clinically manifest as a cervical radiculopathy (single nerve root injury). Also, problems with the SCOT instrumentation led to the loss of some data; however, the affected segments were not immediately adjacent to the most injured levels.

CONCLUSIONS

These results add to our understanding of compressive cervical spine injury mechanisms with lateral eccentricities and provide data for preventing and treating injuries in this important loading mode. For example, as high eccentricity impacts produce lower canal occlusions indicating a lower risk of neurologic impairment, these may be preferable to low eccentricity impacts when the direction of loading can be controlled by injury prevention measures. The classification functions developed in the present study enhance our understanding of the injury mechanism of compression combined with lateral bending. With additional specimens tested at varying eccentricities, these data may be used to definitively understand the spectrum of cervical spine injuries produced by compression with combined lateral bending. Further understanding this injury mechanism can aid surgeons in recognizing these injuries and in planning surgical procedures and researchers in developing prevention approaches.

ACKNOWLEDGEMENTS

We are grateful for the financial support from the Natural Sciences and Engineering Research Council, and for the Applied Biomechanics Laboratory of the University of Washington for loan of the spinal canal occlusion transducer.

REFERENCES

AFIFI, A. A. and V. CLARK, (1996). Computer-Aided Multivariate Analysis. Chapman & Hall, London.

ALLEN, B. L., JR., R. L. FERGUSON, T. R. LEHMANN and R. P. O'BRIEN, (1982). A mechanistic classification of closed, indirect fractures and dislocations of the lower cervical spine. Spine (Phila Pa 1976) 7(1), 1-27.

AMEVO, B., D. WORTH and N. BOGDUK, (1991). Instantaneous axes of rotation of the typical cervical motion segments: a study in normal volunteers. Proceedings of the Clinical Biomechanics, 111-117.

BAHLING, G. S., R. T. BUNDORF, G. S. KASPZYK, E. A. MOFFATT, K. F. ORLOWSKI and J. E. STOCKE, (1990). Rollover and drop tests - the influence of roof strength on injury mechanics using belted dummies. Proceedings of the. Orlando FL, 34th Stapp Car Crash Conference, 101-112.

BAILES, J. E., J. M. HERMAN, M. R. QUIGLEY, L. J. CERULLO and P. R. MEYER, (1990). Diving injuries of the cervical spine. Surgical Neurology 34(3), 155-8.

CARTER, J. W., (2002). Compressive cervical spine injury: the effect of injury mechanism on structural injury pattern and neurologic injury potential. PhD thesis, University of Washington, Seattle WA.

CARTER, J. W., G. S. KU, D. J. NUCKLEY and R. P. CHING, (2002). Tolerance of the cervical spine to eccentric axial compression. Proceedings of the Stapp Car Crash Journal, SAE, 441-59.

CHRISMAN, O. D., G. A. SNOOK, J. M. STANITIS and V. A. KEEDY, (1965). Lateral-flexion neck injuries in athletic competition. Proceedings of the Journal of the American Medical Association, 613-5.

CROWELL, R. R., M. SHEA, W. T. EDWARDS, P. L. CLOTHIAUX, A. A. WHITE and W. C. HAYES, (1993). Cervical injuries under flexion and compression loading. Journal of Spinal Disorders 6(2), 175-181.

EDWARDS, W. T. (1998). Principles of cervical spine biomechanical testing. <u>Frontiers in head and neck trauma</u>. N. Yoganandan. Burke VA, IOS Press**:** 217-31.

EPPINGER, R., E. SUN, S. KUPPA and R. SAUL, (2000). Supplement: Development of Improved Injury Criteria for the Assessment of Advanced Automotive Restraint Systems. Proceedings of the, National Highway Traffic Safety Administration, 40 pages.

GADD, C. W., C. C. CULVER and A. M. NAHUM, (1971). A study of responses and tolerances of the neck. Proceedings of the. Coronado CA, 15th Stapp Car Crash Conference, 256-268.

HALLIDAY, A. L., B. R. HENDERSON, B. L. HART and E. C. BENZEL, (1997). The management of unilateral lateral mass/facet fractures of the subaxial cervical spine: the use of magnetic resonance imaging to predict instability. Spine (Phila Pa 1976) 22(22), 2614-21.

HARTWIG, E., A. KETTLER, M. SCHULTHEISS, L. KINZL, L. CLAES and H. J. WILKE, (2004). In vitro low-speed side collisions cause injury to the lower cervical spine but do not damage alar ligaments. European Spine Journal 13(7), 590-7. Epub 2004 Jun 22.

HORSCH, J. D., D. C. SCHNEIDER, C. K. KROELL and F. D. RAASCH, (1979). Response of Belt Restrained Subjects in Simulated Lateral Impact.

HU, J., K. H. YANG, C. C. CHOU and A. I. KING, (2008). A numerical investigation of factors affecting cervical spine injuries during rollover crashes. Spine (Phila Pa 1976) 33(23), 2529-35.

KALLIERIS, D., A. RIZZETTI, R. MATTERN, J. THUNNISSEN and M. PHILIPPENS, (1996). Cervical human spine loads during traumatomechanical investigations. In Proceedings of the International Research Council on the Biomechanics of Impact Conference (IRCOBI). Dublin, Ireland.

KALLIERIS, D. and G. SCHMIDT, (1990). Neck response and injury assessment using cadavers and the US-SID for far-side lateral impacts of rear seat occupants with inboard-anchored shoulder belts. Proceedings of the. Orlando FL, 34th Stapp Car Crash Conference, 93-100.

KEARNEY, P. A., S. A. RIDELLA, D. C. VIANO and T. E. ANDERSON, (1988). Interaction of contact velocity and cord compression in determining the severity of spinal cord injury. Journal of Neurotrauma 5(3), 187-208.

KETTLER, A., K. FRUTH, E. HARTWIG, L. CLAES and H. J. WILKE, (2004). Correlation between neck injury risk and impact severity parameters in low-speed side collisions. Spine (Phila Pa 1976) 29(21), 2404-9.

KLAUS, G. and D. KALLIERIS, (1983). Side impact - a comparison between HSRI, APROD and Hybrid II dummies and cadavers.

LEE, S. H. and J. K. SUNG, (2009). Unilateral lateral mass-facet fractures with rotational instability: new classification and a review of 39 cases treated conservatively and with single segment anterior fusion. Journal of Trauma 66(3), 758-67.

LIFESO, R. M. and M. A. COLUCCI, (2000). Anterior fusion for rotationally unstable cervical spine fractures. Spine (Phila Pa 1976) 25(16), 2028-34.

MAIMAN, D. J., N. YOGANANDAN and F. A. PINTAR, (2002). Preinjury cervical alignment affecting spinal trauma. Journal of Neurosurgery Spine 97(1), 57-62.

MCELHANEY, J., R. G. SNYDER, J. D. STATES and M. A. GABRIELSEN, (1979). Biomechanical Analysis of Swimming Pool Neck Injuries. Proceedings of the. San Diego CA, 23rd Stapp Car Crash Conference, 47-53.

MCINTOSH, A. S., D. KALLIERIS and B. FRECHEDE, (2007). Neck injury tolerance under inertial loads in side impacts. Accident Analysis and Prevention 39(2), 326-33. Epub 2006 Oct 17.

MERTZ, H. J., V. R. HODGSON, L. M. THOMAS and G. W. NYQUIST, (1978). An assessment of compressive neck loads under injury-producing conditions. The Physician and Sports Medicine 6(11), 95-106.

MERTZ, H. J., A. L. IRWIN and P. PRASAD, (2003). Biomechanical and scaling bases for frontal and side impact injury assessment reference values. Proceedings of the Stapp Car Crash Journal, 155-88.

MERTZ, H. J. and L. M. PATRICK, (1971). Strength and response of the human neck. Proceedings of the. San Diego CA, 15th Stapp Car Crash Conference.

MOFFATT, E. A., E. R. COOPER, J. J. CROTEAU, K. F. ORLOWSKI, D. R. MARTH and J. W. CARTER, (2003). Matched-pair rollover impacts of rollcaged and production roof cars using the controlled rollover impact system (CRIS). Proceedings of the. Detroit MI, SAE World Congress.

MORONEY, S. P., A. B. SCHULTZ, J. A. A. MILLER and G. B. J. ANDERSSON, (1988). Load-Displacement properties of lower cervical spine motion segments. Journal of Biomechanics 21(9), 769-779.

MYERS, B. S. and B. A. WINKELSTEIN, (1995). Epidemiology, classification, mechanism, and tolerance of human cervical spine injuries. Critical reviews in biomedical engineering 23(5-6), 307-409.

NIGHTINGALE, R. W., V. CAROL CHANCEY, D. OTTAVIANO, J. F. LUCK, L. TRAN, M. PRANGE and B. S. MYERS, (2007). Flexion and extension structural properties and strengths for male cervical spine segments. Journal of Biomechanics 40(3), 535-42.

NIGHTINGALE, R. W., J. H. MCELHANEY, W. J. RICHARDSON and B. S. MYERS, (1996). Dynamic response of the head and cervical spine to axial impact loading. Journal of Biomechanics 29(3), 307-318.

NYQUIST, G. W., P. C. BEGMAN, A. I. KING and H. J. MERTZ, (1980). Correlation of field injuries and GM hybrid III dummy responses for lap-shoulder belt restraint. Journal of Biomechanical Engineering 102(2), 103-9.

PATRICK, L. M. and C. C. CHOU, (1976). Response of the Human Neck in Flexion, Extension and Lateral Flexion. Proceedings of the. Warrendale, PA, Vehicle Research Institute (report no. VRI-7.3), 171 pages.

PINTAR, F. A., N. YOGANANDAN, M. PESIGAN, J. REINARTZ, A. J. SANCES and J. F. CUSICK, (1995). Cervical vertebral strain measurements under axial and eccentric loading. Journal of Biomechanical Engineering 117(4), 474-478.

PRASAD, P. and R. DANIEL, (1984). A Biomechanical Analysis of Head, Neck, and Torso Injuries to Child Surrogates Due to Sudden Torso Acceleration. Proceedings of the. Chicago IL, 28th Stapp Car Crash Conference, 25-40.

PRZYBYLA, A. S., D. SKRZYPIEC, P. POLLINTINE, P. DOLAN and M. A. ADAMS, (2007). Strength of the cervical spine in compression and bending. Spine (Phila Pa 1976) 32(15), 1612-20.

RAYNAK, G. C., (2000). Cervical spine injury potential resulting from sagittal plane inertial loading. PhD thesis, University of Washington, Seattle WA.

RAYNAK, G. C., D. J. NUCKLEY, A. F. TENCER and R. P. CHING, (1998). Transducers for dynamic measurement of spine neural-space occlusions. Journal of Biomechanical Engineering 120(6), 787-791.

ROAF, R., (1963). Lateral flexion injuries of the cervical spine. Proceedings of the Journal of Bone and Joint Surgery 36-8.

SCHAAF, R. E., J. A. GEHWEILER, M. D. MILLER and B. POWERS, (1978). Lateral hyperflexion injuries of the cervical spine. Proceedings of the Skeletal Radiology, 73-8.

SCHER, A. T., (1981). Radiological assessment of lateral flexion injuries of the cervical spine. South African Medical Journal 60(26), 983-5.

SELECKI, B. R. and H. B. L. WILLIAMS, (1970). Injuries to the cervical spine and cord in man. Australasian Medical Publishing Company Ltd., Sydney NSW, Australia.

SHARMA, S., (1996). Applied Multivariate Techniques. John Wiley & Sons Inc., New York NY.

SHEA, M., W. T. EDWARDS, A. A. WHITE and W. C. HAYES, (1991). Variations of stiffness and strength along the human cervical spine. Journal of Biomechanics 24(2), 95-107.

SOUTHERN, E. P., T. R. OXLAND, M. M. PANJABI and J. S. DURANCEAU, (1990). Cervical spine injury patterns in three modes of high-speed trauma: a biomechanical porcine model. Journal of Spinal Disorders 3(4), 316-328.

TATOR, C. H., C. F. PROVVIDENZA, L. LAPCZAK, J. CARSON and D. RAYMOND, (2004). Spinal injuries in Canadian ice hockey: documentation of injuries sustained from 1943-1999. Canadian Journal of Neurological Sciences 31(4), 460-6.

THOMPSON, W. L., I. G. STIELL, C. M. CLEMENT and R. J. BRISON, (2009). Association of injury mechanism with the risk of cervical spine fractures. Canadian Journal of Emergency Medicine 11(1), 14-22.

TOOMEY, D. E., (2012). Cervical spine tolerance and response in compressive loading modes including combined compression and lateral bending. PhD thesis, Wayne State University, Detroit MI.

TOOMEY, D. E., M. J. MASON, W. N. HARDY, K. H. YANG, J. M. KOPACZ and C. VAN EE, (2009). Exploring the role of lateral bending postures and asymmetric loading on cervical spine compression responses. In Proceedings of the International Mechanical Engineering Congress & Exposition. Lake Buena Vista FL.

TORG, J. S., J. T. GUILLE and S. JAFFE, (2002). Injuries to the cervical spine in American football players. Journal of Bone and Joint Surgery, American volume 84-A(1), 112-22.

VAN TOEN, C., (2013). Biomechanics of cervical spine and spinal cord injury under combined axial compression and lateral bending loading. Ph.D. thesis, University of British Columbia, Vancouver.

VAN TOEN, C., A. D. MELNYK, J. STREET, T. R. OXLAND and P. A. CRIPTON, (2014a). The effect of lateral eccentricity on failure loads, kinematics, and canal occlusions of the cervical spine in axial impact *Journal of Biomechanics* 47(5), 1164-72.

VAN TOEN, C., J. STREET, T. R. OXLAND and P. A. CRIPTON, (2014b). Cervical spine injuries and flexibilities following axial impacts with lateral eccentricities *in review at European Spine Journal*.

WALKER, L. B., E. H. HARRIS and U. R. PONTIUS, (1973). Mass, volume, center of mass, and mass moment of inertia of head and head and neck of human body. Proceedings of the. Oklahoma City OK, 17th Stapp car crash conference. SAE 525-537.

WHITE, A. A. and M. M. PANJABI, (1990). Clinical biomechanics of the spine. J.B. Lippincott Company, New York NY.

YOGANANDAN, N., J. HUMM, F. A. PINTAR, C. E. WOLFLA and D. J. MAIMAN, (2011). Lateral neck injury assessments in side impact using post mortem human subject tests. In Proceedings of the 55th Annals of Advances in Automotive Medicine (AAAM) Conference. Paris, France.

YOGANANDAN, N., F. A. PINTAR, D. J. MAIMAN, M. PHILIPPENS and J. WISMANS, (2009). Neck forces and moments and head accelerations in side impact. Traffic Injury Prevention 10(1), 51-7.

ZHU, Q., C. LANE, R. P. CHING, J. D. GORDON, C. G. FISHER, M. F. DVORAK, P. A. CRIPTON and T. R. OXLAND, (2008). Translational constraint influences dynamic spinal canal occlusion of the thoracic spine: an in vitro experimental study. Journal of Biomechanics 41(1), 171-9. Epub 2007 Aug 20.

ZHU, Q., J. OUYANG, W. LU, H. LU, Z. LI, X. GUO and S. ZHONG, (1999). Traumatic instabilities of the cervical spine caused by high-speed axial compression in a human model. An in vitro biomechanical study. Spine (Phila Pa 1976) 24(5), 440-444.